

## Surface segregation in liquid mixtures with strong interspecies attraction

Mark J. Osborne\* and Daniel J. Lacks†

Department of Chemical Engineering, Case Western Reserve University, Cleveland, Ohio 44106, USA

(Received 3 May 2004; published 30 July 2004)

Simulations are carried out to investigate surface segregation in liquid mixtures with strong interspecies attraction. The simulations show that the majority species of particles segregates to the surface, even if the other species has the lower pure-component surface tension. This behavior is expected in metal-metalloid mixtures, such as Ni-P, and mixtures in which hydrogen bonds can form only between unlike species, such as acetone-chloroform.

DOI: 10.1103/PhysRevE.70.010501

PACS number(s): 61.20.Ja, 68.03.Cd

Concentrations at the surfaces of multicomponent liquids generally differ from the concentrations in the bulk. This surface segregation can have important consequences, in that glasses prepared by cooling such liquids will have the surface segregation locked in. Since many applications involve processes occurring at surfaces, these processes will depend on surface concentrations that differ from the bulk concentrations.

The usual case of surface segregation involves the enrichment at the surface of the species with the lowest surface tension. However, we show here that in systems with strong inter-species attraction, the direction and magnitude of segregation are highly dependent on the bulk concentration.

Strong interspecies attraction occurs in metal-metalloid mixtures (e.g., Ni-P), due to the strong covalent bonding forces between the transition metal  $d$  electrons and the metalloid  $p$  electrons [1]. Strong interspecies attractions also occur in mixtures where hydrogen bonding occurs only between different species (e.g., acetone-chloroform) [2,3].

Before presenting simulation results that demonstrate the concentration-dependent effects, we discuss surface segregation in terms of a mean-field lattice model in order to anticipate the interesting regions of parameter space. A two component system with bulk concentration  $x_A$  is modeled on a lattice with a coordination number of  $z$ ; the interaction energy for nearest neighbors of components  $i$  and  $j$  is denoted  $E_{ij}$ . Following Guggenheim [4], the surface is considered as a monolayer in equilibrium with the bulk, with  $z'$  interactions between the monolayer and the bulk. The relevant quantities that affect surface segregation are  $\chi = (E_{AB} - E_{AA}/2 - E_{BB}/2)$ , which is the enthalpy of mixing per molecule, and  $a\Delta\gamma$ , where  $\Delta\gamma = \gamma_A - \gamma_B$  is the difference in the pure component surface tensions and  $a$  is the surface area covered by one lattice site at the surface.

Some pertinent results of the mean-field lattice model are summarized in Fig. 1. In Fig. 1 the diagonal solid line represents values of  $\chi$  and  $a\Delta\gamma$  for which the concentration in the surface monolayer is the same as in the bulk. The region of parameter space to the right of the solid line represents enrichment in  $B$ , and the region to the left of the solid line

represents enrichment in  $A$ . The balance between the effects of  $a\Delta\gamma$  and  $\chi$  is concentration dependent: the slope of the line that separates  $A$  enrichment from  $B$  enrichment is  $z'/(1-2x_A)$  and ranges from 1 in the limit  $x_A \rightarrow 0$ , to  $\infty$  in the limit  $x_A \rightarrow 0.5$ , to  $-1$  in the limit  $x_A \rightarrow 1$ . Most importantly, there is the potential for a competition between the effects of  $\Delta\gamma$  and  $\chi$ :  $\Delta\gamma$  acts to enrich the surface with the lower surface tension component (i.e., enrichment of component  $B$ , for  $\Delta\gamma > 0$ , enrichment of component  $A$  for  $\Delta\gamma < 0$ ), whereas  $\chi$  acts in a concentration-dependent way (i.e., enrichment of the minority species for  $\chi > 0$ , and enrichment of the majority species for  $\chi < 0$ ).

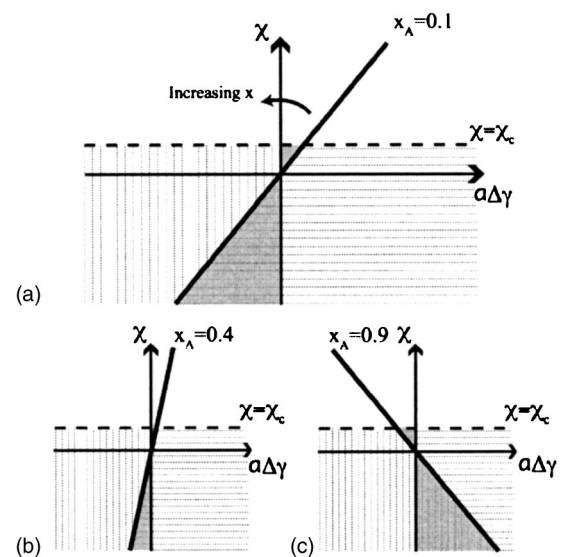


FIG. 1. A map of the parameter space for the Guggenheim model for surface segregation. The solid diagonal line shows values of  $\chi$  and  $a\Delta\gamma$  for which the surface and bulk concentrations are equal. Results for bulk concentrations of component  $A$  of (a) 0.1, (b) 0.4, and (c) 0.9 are given. The region of parameter space to the left of the solid line (vertical hatching) is where the surface is enriched in species  $A$ , and the region to the right of the solid line (horizontal hatching) is where the surface is enriched in species  $B$ . The shaded area is where the surface segregation is in the contrary direction to that which one would expect from the surface tension. The dashed line indicates the critical value of  $\chi$ ,  $\chi_c$  above which bulk phase separation occurs.

\*Electronic address: mjo8@cwru.edu

†Electronic address: djl15@cwru.edu

Thus, the effects of  $\chi$  can in some cases reverse the surface segregation expected on the basis of the pure component surface tensions. This “surface segregation reversal” can occur in principle with both positive and negative  $\chi$ , when the magnitude of  $\chi$  is sufficiently large. The regions of parameter space in which this surface segregation reversal occurs are shaded in Fig. 1. We note the lattice model predicts that surface segregation reversal can never occur in the case of London dispersion forces, which follow the mixing rule  $E_{AB}=(E_{AA}E_{BB})^{1/2}$ .

While in principle both positive and negative  $\chi$  can reverse the effects of the pure component surface tensions, we point out here that only the negative  $\chi$  is likely to be significant in this regard. As  $\chi$  becomes strongly positive, phase separation occurs in the bulk; in this mean-field lattice model, phase separation occurs for  $\chi > ch_c = 2k_B T/z$ . As shown in Fig. 1, this phase separation in the bulk will preclude the surface segregation reversal in most cases for positive  $\chi$ . Therefore, this surface segregation reversal will be observed most readily for negative  $\chi$ .

We carry out simulations to address surface segregation in two systems with strongly attractive interspecies interactions ( $\chi < 0$ ): a metal-metalloid mixture, and a mixture in which hydrogen bonding occurs only between species.

A metal-metalloid system is addressed using the Ni-P model originally created by Stillinger and Weber [5], and modified by Kob and Andersen [6]. The model is a binary Lennard-Jones system with  $\epsilon_{PP}=0.5\epsilon_{NN}$ ,  $\epsilon_{NP}=1.5\epsilon_{NN}$ ,  $\sigma_{PP}=0.88\sigma_{NN}$ , and  $\sigma_{NP}=0.8\sigma_{NN}$ . Both particle types have the mass  $m$  (although the mass does not affect the equilibrium configurations discussed here). The unit of time is  $(m\sigma_{NN}^2/\epsilon_{NN})^{1/2}$  and the unit of energy is  $\epsilon_{NN}$ . This model of Ni-P, with  $x_N=0.8$ , has never been observed to demix—for this reason it has been extensively used in the simulation of supercooled fluids [7,8].

The surface tensions of the pure components Ni,P can be found by reference to the reduced surface tension curve  $\gamma_r(T_r)$ , where  $\gamma=\gamma_r(T_r)\epsilon/\sigma^2$  and the quantity  $\gamma_r(T_r)$  decreases monotonically with increasing  $T_r(T_r=k_B T/\epsilon)$  [9,10]. The result is that the surface tension of P is significantly less than the surface tension of Ni, both because  $\epsilon_{NN}/\sigma_{NN}^2 > \epsilon_{PP}/\sigma_{PP}^2$  and because  $\gamma_r(T_r^N) > \gamma_r(T_r^P)$  (this latter effect occurs because  $k_B T/\epsilon_{NN} < k_B T/\epsilon_{PP}$ ).

Simulations of the Ni-P mixture are performed for a cluster numbering 4000 particles. A reduced time step  $\tau=0.003$  and a reduced temperature of  $T=0.55$  are used for all simulations. A radial harmonic potential that acts only at radii exceeding  $10\sigma_{NN}$  (which is outside the condensed phase) is added to prevent the slow evaporation of the cluster; we verified that the position of this containing potential does not influence the cluster. The vapor phase is very sparse at this temperature and thus exerts a negligible force on the cluster, which may be considered to be at low pressure. Each simulation is run for at least 200 000 steps to establish equilibrium. The temperature is set by means of a Gaussian thermostat, and every 500 steps a new distribution of velocities is drawn. We also ran Monte Carlo simulations of the same system, and equivalent results were obtained.

Simulations of the Ni-P mixture were carried out for differing concentrations of Ni and P atoms. Profiles for the local

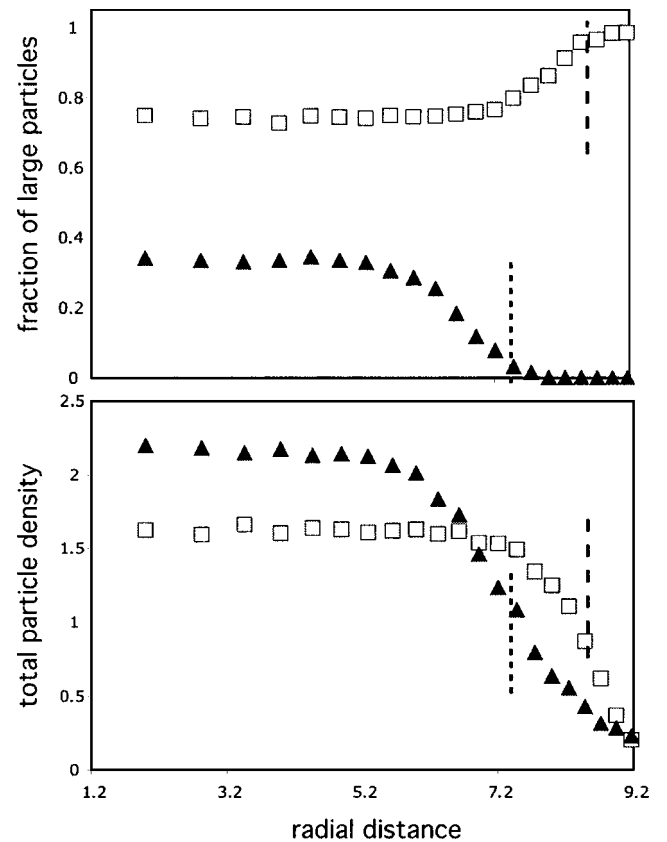


FIG. 2. Simulation results for the Ni-P system; profiles of the local number fraction of Ni and the local total particle number density as a function of radial distance from the center of the cluster. The overall proportions of particles present are  $x_{Ni}=0.8$  ( $\square$ ), and  $x_{Ni}=0.2$  ( $\blacktriangle$ ). The dotted lines mark the surface (defined as where the particle density has fallen to 50% of the bulk value).

number fraction of Ni as a function of radial distance from the cluster center are given in Fig. 2. The total particle density profile is also plotted to show the position of the surface, defined as where the particle profile has fallen to one-half the bulk value; the position of the surface is marked by a dashed line. The simulated temperature is above the glass transition temperature, so the liquid cluster adopts the form of a spherical droplet. We verified that particles within the cluster diffuse significantly over the timescale of the simulation.

For the overall number fraction of Ni,  $x_N=0.2$ , the local number fraction in the interior remains constant at about 0.2, whereas in the surface region there is a substantial enrichment of the P atoms. The enrichment takes place at the surface but in a region of significant particle density (i.e., not only in the tail of the density distribution). Since  $\gamma_P < \gamma_N$ , this surface enrichment of the P atoms concurs with the expectation based on the pure component surface tensions.

In contrast, for  $x_N=0.8$  there is a substantial enrichment of the Ni atoms. This surface enrichment of Ni occurs despite the fact that Ni has the larger pure component surface tension.

We also ran simulations at other number fractions. The majority particle species was found to be enriched at the surface in each case—simulations were carried out showing this general principle remains true even for Ni-P  $x_N=0.45$ ,

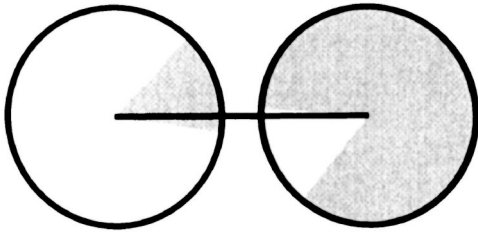


FIG. 3. Schematic of the particle interactions in the polar non-associating system. Two particles of different types are shown associated here. The missing segment of the circle represents the angular range over which the particle can associate with a particle of the different species.

and  $x_N=0.55$  and negligible surface enrichment is observed for  $x_N=0.5$ . So the Ni-P mixture behaves qualitatively like the Guggenheim lattice model for  $\chi < 0$  and  $\Delta\gamma \sim 0$ . For the Ni-P mixture it is true that  $\chi < 0$ , however the surface tensions of the pure Ni,P components are significantly different, so one would expect to see segregation when  $x_N=0.5$ . Deviations from the lattice model are expected, due to the different, and nonadditive, sizes of the Ni,P atoms and also the fact that the surface is not a sharp monolayer in the simulation.

The other system that is simulated is a mixture in which hydrogen bonding occurs only between unlike species (see Fig. 3). In this model, the state of each particle is described by an orientation in addition to a position. All particles interact with an orientation-independent van der Waals interaction. In addition, interspecies interactions include an orientation-dependent hydrogen bonding interaction. The detailed pair interactions  $\Phi_{\alpha\beta}(r_{ij}, \theta_i, \theta_j)$  are given by

$$\Phi_{\alpha\beta}(r_{ij}, \theta_i, \theta_j) = u_{\text{vdW}}(r_{ij}) + (1 - \delta_{\alpha\beta})u_{\text{hb}}(r_{ij}, \theta_i, \theta_j)$$

$$u_{\text{vdW}} = \begin{cases} \infty & \text{if } 0 < r_{ij} < 1 \\ -\epsilon & \text{if } 1 \leq r_{ij} < \sigma \\ 0 & \text{if } r_{ij} \geq \sigma \end{cases} \quad (1)$$

$$u_{\text{hb}} = \begin{cases} -\epsilon_{\text{hb}} & \text{if } 1 < r_{ij} < r_c, \theta_i < \theta_c, \theta_j < \theta_c \\ 0 & \text{otherwise} \end{cases},$$

where  $\sigma=1.5$ ,  $r_c=1.2$ ,  $\theta_c=27^\circ$  and  $\alpha, \beta$  denote the types of interacting particles. The angle  $\theta_i$  is the angle between the orientation vector of particle  $i$  and the vector connecting particles  $i$  and  $j$ . This model is based on a model used to examine the phases of a hydrogen bonded self-associating fluid (acetic acid) [11]. The parameters are chosen such that each particle will likely form hydrogen bonds with only one other particle. In this model the intraspecies interactions are identical—the only property that differentiates the two species is that they can form hydrogen bonds only with the other species. Thus, simulating the  $x_A=0.8$  system is identical to simulating the  $x_A=0.2$  system with a relabeling of particles.

The interspecies hydrogen bonding system was simulated by carrying out Monte Carlo simulations on clusters of 4000 particles in the 80:20 ratio at a temperature of  $T=0.55$ . At this temperature, the system behaves as a liquid. The simu-

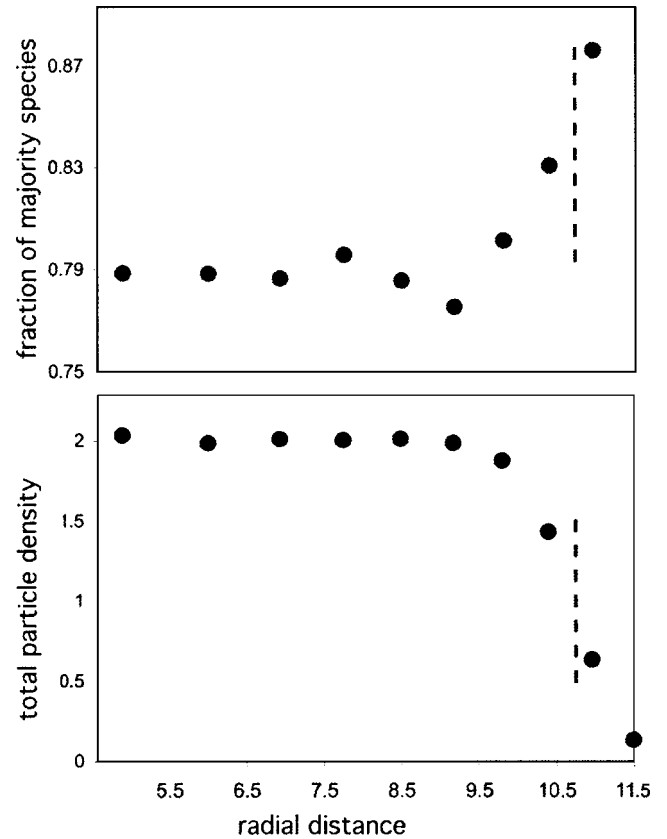


FIG. 4. Simulation results for the interspecies hydrogen bonding system with interaction energy  $\epsilon_{\text{hb}}=5$ ; profiles of the local number fraction of majority particle species and the local total particle density as a function of radial distance from the center of the cluster. The dotted lines mark the surface (defined as where the particle density has fallen to 50% of the bulk value).

lations are carried out for a range of the strength of the hydrogen bonding interaction  $\epsilon_{\text{hb}}$ . For  $\epsilon_{\text{hb}} \leq 1$ , the effect of the hydrogen bonding is negligible (due to the small orientation range in which hydrogen bonds can form). As  $\epsilon_{\text{hb}}$  increases, the lifetime of hydrogen bonded pairs increases (though the system remains liquid).

For  $\epsilon_{\text{hb}} \geq 2$  the majority species of particle starts segregating to the surface. The results for  $\epsilon_{\text{hb}}=5$  are given in Fig. 4. Since simulating the  $x_A=0.8$  system is identical to simulating the  $x_A=0.2$  system with a relabeling of particles, reversing the particle proportions produces the “same” result in that the majority species again segregates to the surface. Thus, surface segregation, whose direction depends on the bulk concentration, persists even when the attractive interspecies interactions are highly directional.

The technological importance of metal alloy surfaces has led to much work on the composition of the surface layers, in Refs. [12–18], of crystalline alloys. However, the issues involved in crystalline alloy can be very different than in liquid alloys. For example, surface segregation is dependent on the particular surface orientation [19]. Also the disparity in the atom sizes is less important for disordered liquids, and especially in our simulations—in the case of the Ni-P system the disparity in size is not great, while in the hydrogen-bonded mixture there is no difference in particle sizes.

In contrast to the situation for crystalline systems, experimental determination of the composition of liquid surfaces is difficult, with results generally obtained indirectly (using surface tension, neutron reflectivity, and electron diffraction measurements) and requiring significant interpretation. Most experiments on surface segregation in liquids have been carried out on water-alcohol mixtures, which exhibit the usual surface segregation effect (due to the difference in surface tensions), the alcohol enriches the surface at all concentrations [20]. Similarly, experimental studies on liquid metal alloys have always found the lowest surface tension component segregating to the surface [21].

Usually in liquid metal alloys there is a surface monolayer composed almost completely of the low surface tension component [21]. However, experiments on the liquid alloy mixture Bi-In with  $x_{\text{Bi}}=0.22$  show that the low surface tension component (bismuth) segregates preferentially to the surface, with a surface concentration of  $x_{\text{Bi}}=0.35$  (i.e., less segregation than usual). Thus, this experiment shows that the strongly attractive heteratomic interaction between Bi and In (i.e.,  $\chi < 0$ ) is at least capable of partly offsetting the usual surface tension effect.

The present analysis can help guide experimental investigations to detect surface segregation reversal. The Guggenheim model (see Fig. 1) shows that the region of  $\chi-\Delta\gamma$  parameter space, where surface segregation occurs in a direction contrary to that suggested by surface tension, is largest in the dilute limit. Thus a reversal in the usual surface segregation direction is most likely to be observed in experiments carried out at low concentrations of the low surface tension component.

It is instructive to develop a simple picture of the physics driving the concentration-dependent surface segregation. Particles at the surface have fewer neighbors and hence fewer interactions than particles in the bulk. So if the enthalpy of mixing is nonzero, particles at the surface make a smaller contribution to the effective enthalpy of mixing than particles in the bulk. Supposing the surface tensions of the pure components are equal, then a mixture can lower its overall free energy by altering the composition of the bulk to minimize the mixing enthalpy despite the resulting increase in the enthalpy of mixing at the surface. Thus if  $\chi < 0$ , the bulk becomes marginally more mixed and the surface demixes so the majority species segregates to the surface, whereas for  $\chi > 0$  the reverse occurs. In general, when the surface tensions of the pure components are not equal, the concentration dependent effect may oppose (or reinforce) the usual tendency of the component with the lowest surface tension to segregate to the surface.

In summary, simulations and theoretical analysis suggest that surface segregation in liquid mixtures with strong inter-species interactions depends on the concentration of the particles in the bulk, rather than just on the surface tensions of the separate pure components. Our simulations suggest that candidates for this concentration-dependent surface segregation include metal-metalloid mixtures (e.g., Ni-P) and mixtures where hydrogen bonds form only between unlike species.

Funding for this project was provided by the National Science Foundation (Grant No. DMR-0324396).

- 
- [1] C. Hausleitner and J. Hafner, Phys. Rev. B **47**, 5689 (1993).  
 [2] M. Kamlet, J. M. Abboud, M. H. Abraham, and R. W. Taft, J. Org. Chem. **48**, 2877 (1983).  
 [3] J. Smith, H. C. V. Ness, and M. Abbott, *Introduction to Chemical Engineering Thermodynamics*, 5th ed. (McGraw-Hill, New York, 1996).  
 [4] E. Guggenheim, *Mixtures* (Oxford University Press, Oxford, 1952).  
 [5] T. Weber and F. Stillinger, Phys. Rev. B **31**, 1954 (1985).  
 [6] W. Kob and H. C. Andersen, Phys. Rev. Lett. **73**, 1376 (1994).  
 [7] S. Sastry, P. G. Debenedetti, and F. H. Stillinger, Nature (London) **393**, 556 (1998).  
 [8] D. J. Lacks, Phys. Rev. Lett. **87**, 225502 (2001).  
 [9] M. Mecke, J. Winkelmann, and J. Fischer, J. Chem. Phys. **107**, 9264 (1997).  
 [10] J. Errington, Phys. Rev. E **67**, 012102 (2003).  
 [11] J. K. Singh and D. A. Kofke, Preprint (2003).  
 [12] U. Bardi, Rep. Prog. Phys. **57**, 939 (1994).  
 [13] M. Polak and L. Rubinovich, Surf. Sci. Rep. **38**, 127 (2000).  
 [14] G. Treglia, B. Legrand, F. Ducastelle, A. Saul, C. Gallis, I. Meunier, C. Mottet, and A. Senhsji, Comput. Mater. Sci. **15**, 196 (1999).  
 [15] B. Good and G. Bozzolo, Surf. Sci. **507-510**, 730 (2002).  
 [16] J. Luyten, S. Helfensteyn, and C. Creemers, Appl. Surf. Sci. **212-213**, 833 (2003).  
 [17] S. Helfensteyn, J. Luyten, L. Feyaerts, and C. Creemers, Appl. Surf. Sci. **212-213**, 844 (2003).  
 [18] D. B. Miracle, J. Non-Cryst. Solids **317**, 40 (2003).  
 [19] C. Treglia and B. Legrand, Phys. Rev. B **35**, 4338 (1987).  
 [20] G. Raina, C. U. Kulkarni, and C. R. Rao, J. Phys. Chem. A **105**, 10204 (2001).  
 [21] E. Dimasi, H. Tostman, O. Shpyrkp, P. Huber, B. Ocko, P. Pershan, M. Deutsch, and L. Berman, Phys. Rev. Lett. **86**, 1538 (2001).